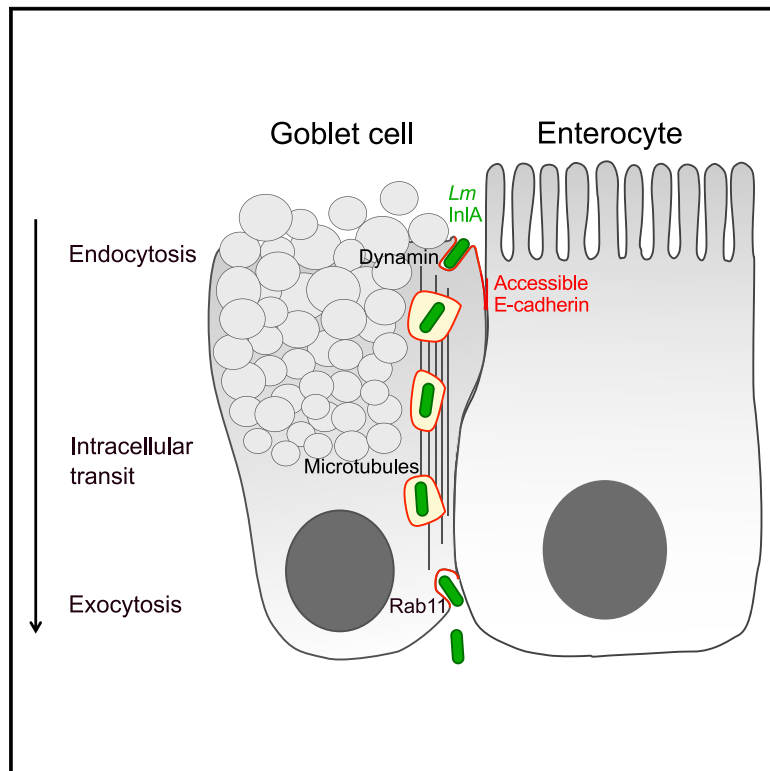


Current Biology

Live Imaging Reveals *Listeria* Hijacking of E-Cadherin Recycling as It Crosses the Intestinal Barrier

Graphical Abstract



Authors

Minhee Kim, Cindy Fevre,
Morgane Lavina, Olivier Disson,
Marc Lecuit

Correspondence

marc.lecuit@pasteur.fr

In Brief

Kim et al. develop an intraluminal microinjection-based intestinal organoid model of *Listeria* infection, which allows real-time imaging. *Listeria* specifically translocates through goblet cells, on which each receptor Ecad is luminally exposed. *Listeria* transcytoses within its membrane internalization vacuole, hijacking Rab11-mediated Ecad recycling.

Highlights

- *Listeria* translocates across organoid goblet cells in an InlA-Ecad-dependent manner
- Real-time imaging reveals *Listeria* transcytosis
- Ecad endocytosis is involved in *Listeria* entry and microtubules in translocation
- *Listeria* hijacks Rab11-dependent Ecad recycling for transcytosis



Report

Live Imaging Reveals *Listeria* Hijacking of E-Cadherin Recycling as It Crosses the Intestinal Barrier

Minhee Kim,^{1,2} Cindy Fevre,^{1,2} Morgane Lavina,^{1,2} Olivier Disson,^{1,2,5} and Marc Lecuit^{1,2,3,4,5,6,*}¹Biology of Infection Unit, Institut Pasteur, Paris, France²Inserm U1117, Paris, France³Necker-Enfants Malades University Hospital, Division of Infectious Diseases and Tropical Medicine, Institut Imagine, APHP, Université de Paris, Paris, France⁴Institut Universitaire de France (IUF), Paris, France⁵Senior author⁶Lead Contact*Correspondence: marc.lecuit@pasteur.fr<https://doi.org/10.1016/j.cub.2020.11.041>

SUMMARY

Listeria monocytogenes is a foodborne bacterial pathogen that causes human listeriosis, a severe systemic infection.¹ Its translocation across the intestinal epithelium is mediated by the interaction of internalin (InIA), a *Listeria* surface protein, with its host-species-specific receptor E-cadherin (Ecad).^{2–5} It occurs through goblet cells, on which Ecad is lumenally accessible,⁶ via an unknown mechanism. In the absence of cell lines recapitulating this phenotype *in vitro*, we developed an *ex vivo* experimental system, based on the intraluminal microinjection of *Listeria* in untreated, pharmacologically treated, and genetically modified intestinal organoids. Using both live light-sheet microscopy and confocal imaging, we show that *Listeria* translocates through goblet cells within a membrane vacuole in an InIA- and microtubule-dependent manner. As Ecad undergoes constant apical-basal recycling,^{7,8} we hypothesized that *Lm* may transit through goblet cells by hijacking Ecad recycling pathway. Indeed, *Listeria* is stuck at goblet cell apex when Ecad endocytosis is blocked and remains trapped intracellularly at the basolateral pole of goblet cells when Rab11-dependent Ecad recycling is compromised. Together, these results show that *Listeria*, upon docking onto its lumenally accessible receptor Ecad, hijacks its recycling pathway to be transferred by transcytosis across goblet cells. Live imaging of host-pathogen interactions in organoids is a promising approach to dissect their underlying cell and molecular biology.

RESULTS AND DISCUSSION

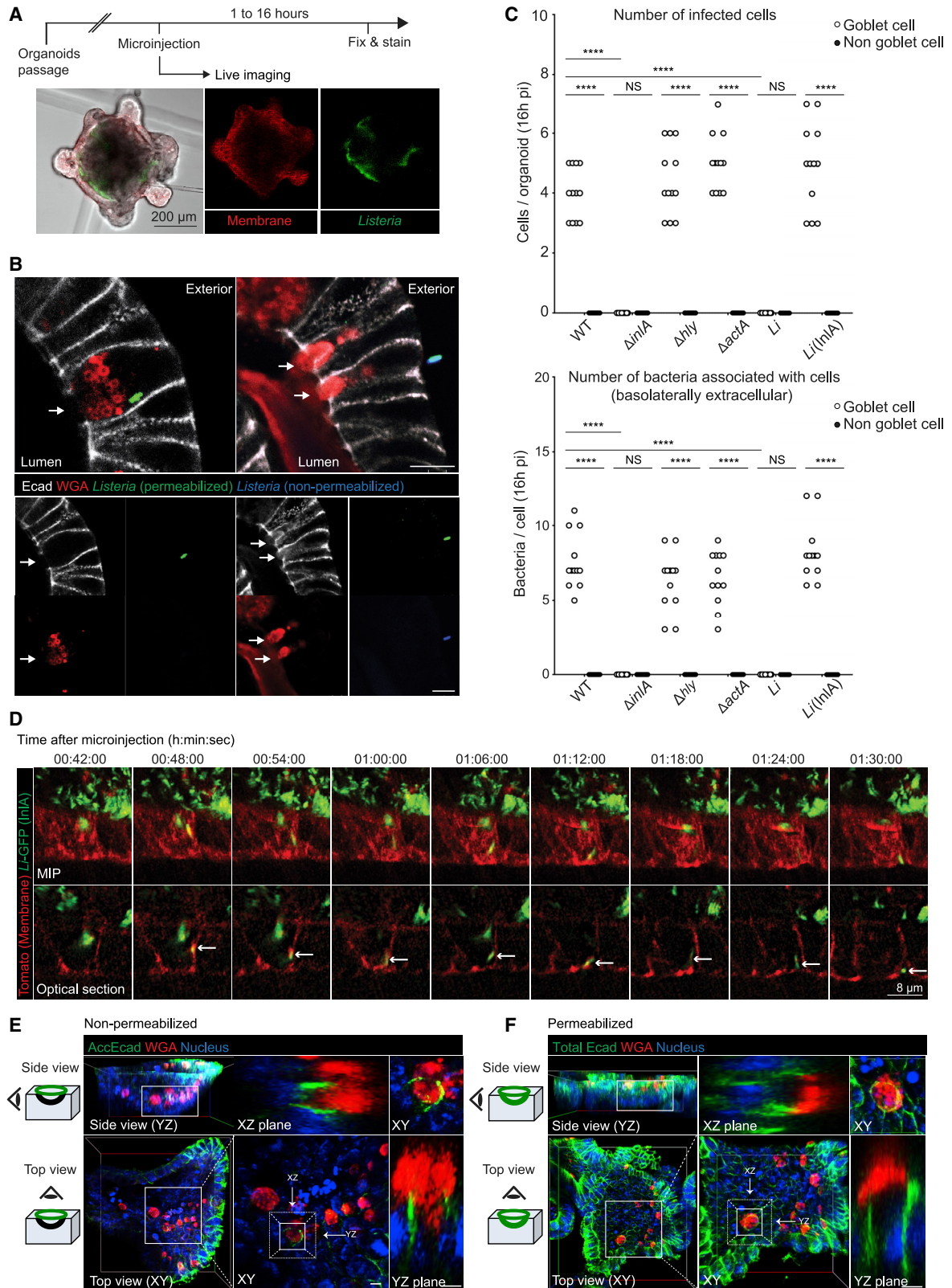
In order to decipher the cell biology mechanisms of *Listeria* translocation across the intestinal epithelium, we developed a genetically amenable experimental system permissive to InIA-Ecad-dependent trans-epithelial crossing. Deciphering the detailed cell biology mechanisms of *Listeria* translocation across the intestinal epithelium *in vivo* would require interfering with cellular pathways that may disrupt its barrier function. Additionally, it would be extremely challenging to capture *Listeria* translocation in real time across intestinal villus epithelium, given its rarity and intestinal peristalsis. Furthermore, no adherent cell, including human colonic cell lines T84, HT29, and Caco-2, displays an apical-basal polarization and apical accessibility of Ecad, which are both critical for *Listeria* InIA-Ecad-dependent trans-epithelial crossing to occur (unpublished data). We therefore set up an *ex vivo* experimental system based on the microinjection of *Listeria* in the lumen of intestinal organoids. Intestinal organoids derive clonally from intestinal stem cells, which give rise to a fully differentiated, polarized intestinal epithelium that forms a so-called “minigut” centered by a lumen and contains

differentiated intestinal cell subtypes.⁹ Intestinal organoids are genetically amenable,^{10–13} can be subjected to pharmacological interventions,¹⁴ and can also be imaged both fixed and alive.^{9,15}

Intestinal Organoids Contain Goblet Cells

We generated intestinal organoids from the small intestine of knockin E16P (E16P KI) mice, in which the endogenous mouse Ecad is punctually modified to express a proline at position 16 of the mature protein in place of a glutamic acid. This modification enables this “humanized” mouse Ecad to interact with InIA and mediate *Listeria* internalization (see STAR Methods).^{1,4,16} As expected,⁹ E16P organoids grown in Matrigel exhibit a fully mature apical-basal polarity and display cell subtype heterogeneity. Organoids intestinal stem cells differentiate into enterocytes (villin⁺), enteroendocrine cells (chromogranin A⁺), goblet cells (wheat germ agglutinin [WGA]⁺/lysozyme^{low}), and Paneth cells (WGA^{low}/lysozyme⁺; Figure S1A). Additionally, and as previously reported,¹⁷ intestinal organoids do not contain M cells (GP2⁺; Figure S1A). As *Listeria* crosses the intestinal barrier via goblet cells *in vivo*, it is important to unambiguously identify this cell subtype in our experimental model. Goblet cells are





(legend on next page)

mucus-secreting cells with a characteristic goblet-shaped cell morphology, in which nucleus location does not align with neighboring enterocytes.¹⁸ Additionally, goblet cells can be identified by immunolabeling of the Muc2 mucin, a major mucus component, following Carnoy hydrophobic fixation.¹⁹ However, Muc2 labeling cannot be applied to our experimental system: Carnoy fixation damages plastic wells in which Matrigel-embedded organoids are located and, more importantly, renders Matrigel opaque. Therefore, we used WGA, which labels mucus by binding to sialic acid and N-acetyl-glucosaminyl carbohydrate residues on mature, modified mucins.^{20,21} WGA-positive cells were co-labeled for cytokeratin-18, which is specifically expressed in goblet cells in the gut (Figure S1B).²² Of note, paraformaldehyde (PFA) fixation can dissolve mucus, resulting in bona fide WGA-negative goblet cells. Therefore, we used the following criteria to identify goblet cells: (1) WGA labeling, (2) goblet-shaped cellular morphology, and (3) misaligned nucleus relative to neighboring cells. When WGA-negative cells strictly met the last two conditions, we also considered them as goblet cells (e.g., in Figure S1D, right).

InIA Is Necessary and Sufficient for *Listeria* Translocation across Intestinal Organoid Goblet Cells

We microinjected 5×10^3 colony-forming units (CFUs) of wild-type (WT) *Lm* into the lumen of mature organoids and investigated bacteria interactions with the intestinal epithelium (Figure 1A). Confocal imaging of intestinal organoids fixed 1 h after microinjection allowed the detection of bacteria both inside and underneath the basolateral pole of goblet cells (Figure 1B; Video S1). Quantification studies 16 h post-infection revealed that bacteria were all located exterior to microinjected organoids, specifically associated with goblet cells, as a result of translocation events (Figure 1C). Of note, the microinjection procedure and/or presence of bacteria in the organoid lumen did not modify the proportion of WGA⁺ cells ($10.87\% \pm 3.07\%$) compared to non-injected organoids ($9.56\% \pm 2.62\%$; Figure S1C). Consistent with our previous *in vivo* studies in humanized mice permissive to InIA-Ecad interaction,^{5,6,16} this

phenotype was strictly InIA dependent. In contrast, it was independent of listeriolysin O (LLO) and ActA, which mediate *Lm* escape from its internalization vacuole and actin-based motility, respectively (Figure 1C). *Li*(InIA) is derived from *L. innocua*, a non-pathogenic *Listeria* species devoid of *L. monocytogenes* virulence factors, which has been genetically modified to express InIA, and enters into cells in an Ecad-dependent manner.²³ Upon microinjection in intestinal organoids lumen, *Li*(InIA) was also located extracellularly at basolateral pole of goblet cells, as wild-type *Lm* (Figures 1C, S1D, and S1E; Video S1). This indicates that *Listeria* crossing of the intestinal epithelium does not require escape from the vacuole and actin-based motility. In some cases, bacteria underneath goblet cells were surrounded with WGA-labeled material, implying that bacteria can translocate with mucus (Figure S1E). Of note, bacteria beneath goblet cells cannot replicate or move within Matrigel, as it contains gentamicin and is bactericidal. Together, these results show that *Listeria* microinjection in the lumen of intestinal organoids allows to faithfully recapitulate *Listeria* translocation across the intestinal epithelium *in vivo*. These results also confirm that InIA is necessary and sufficient to mediate *Listeria* translocation across goblet cells, although LLO and ActA are dispensable,⁶ and justify the use of *Li*(InIA) for further experiments, in order to minimize the potential cytotoxicity of LLO to microinjected organoids.²⁴

Real-Time Imaging of *Listeria* Transcytosis across Intestinal Organoid Epithelium

Despite converging evidence indicating that *Listeria* transcytoses through goblet cells *in vivo*,⁶ live imaging has not been performed to prove it actually occurs, i.e., translocation of a bacterium surrounded by its internalization vacuole. We therefore set up experimental conditions to image in real-time translocation of *Li*-GFP(InIA) across intestinal organoids, in which cell membranes are constitutively red fluorescent (mtd-Tmt; E16P Kl). *Listeria* translocation across the intestinal epithelium is a rare event *in vivo*, as only 3% to 4% of intestinal villi are infected in 45-min-long intestinal ligated loop assays (unpublished data). Moreover, *Lm* translocation across the small intestinal

Figure 1. *Ex Vivo* Intestinal Organoid Model of *Listeria* Infection

(A) Experimental scheme and example of *Listeria* microinjection (details in the STAR Methods).

(B) Example images of *Listeria* translocation (optical section). *Lm* within a goblet cell is shown, fixed 1 h post-microinjection (left panel; goblet cell marked with an arrow). *Lm* basolaterally extracellular beneath a goblet cell is shown (right panel; goblet cells are marked with arrows). See also Video S1. Translocated bacteria were distinguished from the total bacteria by consecutive immunostaining, first against *Lm* without permeabilization followed by tissue permeabilization and labeling (STAR Methods). Scale bars, 10 μ m.

(C) Quantification of *Listeria* translocation. Top: number of cells associated with bacteria either intracellularly or basolaterally extracellularly per organoid is shown. Bottom: number of translocated bacteria per organoid is shown. Counts were performed in 12 organoids for each condition. Two-way ANOVA test; NS, not significant; ****p < 0.0001. See also Figures S1D and S1E and Video S1.

(D) Light-sheet live imaging at indicated time point (top, maximum intensity projection [MIP]; bottom, optical section). Within 12 min, bacteria-containing vesicle reaches the basolateral side of the cells and then exits from the cell in the following time points. Intracellular *Listeria* is surrounded with membrane tomato (arrow). See also Video S2.

(E) Left: scheme depicting detection of lumenally accessible Ecad from side and top view. Organoids were fixed, embedded, sectioned to open the lumen, and immunolabeled from the luminal side without permeabilization. Ecad in the sectioned plane is exposed and thus accessible without permeabilization and stained throughout the cutting plane (marked with green on the drawing). Right: 3D view of opened organoids from the side (top left) and top (bottom left) is shown. Enlargement of boxed area on the left 3D-reconstructed organoids containing goblet cells expressing lumenally accessible Ecad is shown (center and right). Mucus that has been expelled is marked with WGA conjugated with fluorophore. Accessible Ecad surrounds the expelled mucus. Scale bars, 10 μ m. See also Video S3.

(F) Left: scheme depicting detection Ecad from side and top view. Organoids were fixed, embedded, sectioned to open the lumen, permeabilized, and immunolabeled from the luminal side. Total Ecad is stained (marked with green on the drawing). Right: 3D view of opened organoids from the side (top left) and top (bottom left) is shown. Enlargement of boxed area on the left 3D-reconstructed organoids containing goblet cell is shown (center and right). Scale bars, 10 μ m. See also Video S3.

epithelium occurs within 30 min *in vivo*.⁶ The rarity of translocation events requires that entire organoids are scanned to be captured, and this may exceed the time needed for bacterial translocation when using classical confocal imaging. Additionally, laser power has to be minimal to preserve the fluorescence signal of individual bacteria and cell membrane over prolonged imaging. Furthermore, imaging has to be performed at the adequate spatial resolution to track micron-sized bacteria within intestinal organoids, the diameter of which ranges from hundreds to thousands of microns. To accommodate all these experimental requirements, light-sheet microscopy was used, which can image intestinal organoids at least thirty times faster than a regular confocal microscope with minimal phototoxicity. 5×10^3 CFUs of *Li*-GFP(InIA) were microinjected intraluminally into mtd-Tmt; E16P KI organoids. Real-time imaging revealed that a bacterium reached cell basolateral pole surrounded by a cell membrane in less than 12 min. During the following 36 min, the bacterium remained at the basolateral pole of the cell, surrounded by mtd-Tmt signal, and then exited from the cell basolaterally (Figure 1D; Video S2). This allowed to image for the first time *Listeria* transcytosis across the intestinal epithelium directly and unambiguously.

Ecad Is Luminally Accessible on Goblet Cells in Intestinal Organoids

InIA-dependent translocation of *Listeria* specifically through goblet cell (Figures 1B, 1C, S1D, and S1E) suggests that translocation is mediated by InIA interaction with luminally accessible Ecad on goblet cells, as it has been observed *in vivo*.⁶ To assess luminal accessibility of Ecad in organoids, we applied an Ecad antibody directed against its ectodomain (ECCD-2) to the accessible luminal side of fixed and sectioned organoids (Figure 1E). To stain only accessible Ecad, we performed surface immunolabeling without cell permeabilization. Junctional proteins in the sectioned plane are exposed, accessible without permeabilization, and are therefore also labeled. However, junctional proteins located below the cutting plane cannot be labeled in the absence of cell permeabilization, unless they are inherently luminally accessible (Figures 1E and 1F). As expected, given the specific location of InIA-Ecad *Listeria* translocation (Figure 1C), luminally accessible Ecad was detected only on the apical side of mucus-expelling goblet cells in non-permeabilized organoids (Figure 1E; Video S3). In contrast, in permeabilized organoids, Ecad was detected at adherens junctions (AJs), down to the basolateral membrane in all cells, regardless of the subtype (Figure 1F; Video S3). Together, these results indicate that the cells on which Ecad is luminally accessible in intestinal organoids are mucus-expelling goblet cells and that bacteria located beneath the basal pole of goblet cells after intraluminal microinjection have undergone InIA-Ecad-mediated transcytosis. This establishes the specificity of this *ex vivo* experimental system to study the cell

biology of *Listeria* InIA-Ecad translocation across the intestinal epithelium.

Endocytosis and Microtubule Dynamics Are Required for *Listeria* Translocation through Goblet Cells

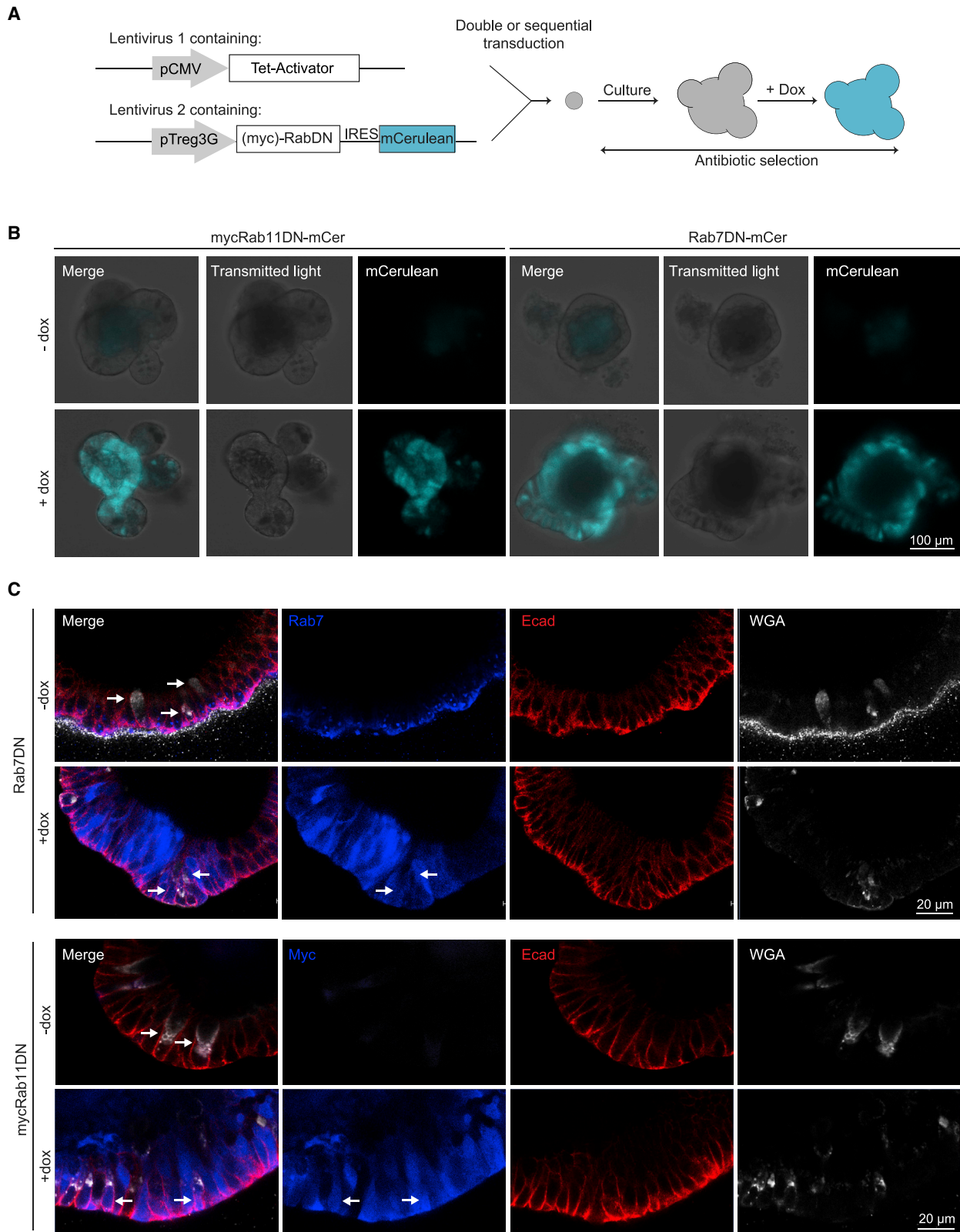
Previous *in vivo* investigations have shown that InIA-Ecad-dependent *Listeria* crossing of the intestinal barrier depends on microtubule and the exocytic machinery.⁶ We therefore hypothesized that *Listeria*, upon its docking on luminally accessible Ecad on goblet cells, hijacks Ecad recycling pathway to cross the intestinal epithelial barrier, from its dynamin-mediated endocytosis⁷ and endosomal trafficking along microtubules²⁵ to its Rab11-dependent release at the cell basolateral pole.^{26,27} Ecad recycling has not been studied in goblet cells, but it is also expected to involve its endocytosis at the apical pole and basolateral recycling in a microtubule-dependent manner. We therefore tested this hypothesis by dissecting the role of Ecad recycling pathway on *Listeria* transcytosis.

In polarized differentiated cells, Ecad, which forms AJs, is endocytosed in a clathrin-dependent manner.⁷ The resulting endosomes are excised from the plasma membrane by the guanosine triphosphatase (GTPase) dynamin.^{28,29} Ecad is trafficked in a microtubule-dependent manner^{25,30,31} and recycled to the basolateral membrane.⁷ To first inhibit Ecad endocytosis, we used dynasore, a dynamin inhibitor that prevents the fission of clathrin- and caveolin-dependent endocytic vacuoles.^{32,33} To inhibit microtubule-based Ecad trafficking, we used colchicine, which blocks microtubule polymerization. In organoids treated 2 h with dynasore, cytosolic endocytic Ecad punctae were drastically reduced (Figure S2C), as previously reported in cultured cells.²⁹ In presence of colchicine, more cells with metaphase-blocked mitoses were observed (Figure 2A), as expected,³⁴ indicating that both drugs are active in our system. Nevertheless, the overall morphology and polarity of the organoids were comparable to non-treated controls (Figure 2A), and we observed no difference in total bacterial association to cells (either apically, intracellularly, or basolaterally; Figure 2B). Yet there was a significant decrease of extracellular translocated bacteria in dynasore- and colchicine-treated organoids, relative to control organoids (Figure 2C). Consistent with a similar total bacterial association to cells in all conditions, accessible Ecad was detected similarly on goblet cells in dynasore- and colchicine-treated conditions (Figures 2D and S2; Video S4), as in untreated organoids (Figure 1E). This suggests that the interaction between *Listeria* and its receptor Ecad is not impaired in dynasore- and colchicine-treated organoids, whereas *Listeria* transcellular transport is blocked within goblet cells. To examine where bacteria were trapped in cells, we investigated their location in three distinct compartments: apically associated to the cell membrane, intracellular, and extracellular at their basal pole. In dynasore-treated organoids, bacteria were mostly apically associated (Figures 2C

(C) Quantification of number of bacteria per organoid in indicated location. Experiments were repeated 2 to 3 times. The results combine all experiments. 27 WT and dynasore-treated organoids and 21 colchicine-treated organoids were counted. Kruskal-Wallis test; comparison to WT; *p < 0.5; **p < 0.01; ****p < 0.0001. See also Figure S3.

(D) Accessible Ecad from the luminal side of the sectioned organoids treated with indicated inhibitors. See also Figure S2 and Video S4.

(E) Confocal images of bacteria trapped inside the goblet cells in each condition (optical section from 3D reconstruction; goblet cells are marked with an arrow). Bacteria are located in apical and central side within the cells in dynasore- and colchicine-treated conditions, respectively. Bacteria are surrounded with a tomato-stained membrane. See also Figure S3 and Video S4.



(legend on next page)

and 2E, dynasore, and S3; Video S4). These bacteria were likely trapped in elongated invaginations of the plasma membrane, as observed both in *Drosophila* and mammalian epithelial cells when dynamin is inhibited.^{35–37} In colchicine-treated organoids, where microtubule dynamics is inhibited, intracellular bacteria were located in the median part of the cells (Figures 2C, 2E, colchicine, and S3; Video S4). In all experimental conditions, intracellular bacteria were surrounded with Tomato red-labeled membrane, indicating that bacteria were within a vacuole (Figure 2E). Together, these results show that, upon InIA-mediated *Listeria* docking to Ecad, Ecad endocytosis is required to complete bacterial internalization into goblet cells, and microtubules dynamics is required for bacterial trans-epithelial transit in a vacuole.

Rab11 Is Required to Complete *Listeria* Intestinal Translocation through Goblet Cells

We next investigated whether recycling of Ecad endosomes is required for *Listeria* InIA-dependent translocation across the intestinal epithelium. Ecad is recycled and trafficked via Rab11-positive recycling endosomes, which recruit the exocytosis machinery.^{8,26,27,38,39} Rab11 is also involved in basolateral sorting of newly synthesized Ecad in polarized mammalian cells *in vitro*.³⁸ The kinetics of Rab11-based trafficking is around 30 min,^{40,41} which fits with our live imaging of *Listeria* crossing the epithelium (Figure 1D; Video S2). Therefore, to perturb Ecad recycling, we targeted Rab11. Because Rab11-null mutations are embryonically lethal in mice^{42,43} and constitutive knockout of Rab11 may be detrimental for the development of intestinal organoids, we generated lentivirus-transduced organoids in which a dominant-negative (DN) and myc-tagged version of Rab11 can be induced by doxycycline. As Rab7-dependent Ecad degradation pathway⁴⁴ is not expected to be involved in bacterial translocation, we also generated lentivirus-transduced organoids in which a dominant-negative Rab7 can be induced to use them as negative controls. To visualize successful transduction and transcription induction, we used a bi-cistronic reporter system where an internal ribosome entry site (IRES) is placed downstream of each DN mutant and upstream of a mCerulean coding sequence (Figures 3A and 3B). Organoids were grown and maintained in presence of antibiotics to select for transduced cells. When organoids were properly formed and mature, doxycycline was added 12–16 h before microinjection to induce the transcription of dominant-negative Rab11 and Rab7 variants Rab11DN and Rab7DN, respectively (Figure 4A). Organoids expressing Rab11DN exhibited cytosolic Ecad punctae that accumulated at basolateral side of epithelial cells compared to control organoids, consistent with a blockade of Ecad release when Rab11 is non-functional (Figure S2C). Induced expression of Rab7DN caused general enrichment of cytosolic Ecad (Figure S2C), and large Ecad

aggregates formed throughout the apical-basal axis (Figure S2C), suggesting that Ecad degradation is affected when Rab7 is non-functional.⁴⁴ However, inducing Rab11 and Rab7 dominant-negative proteins for a short period of time (less than 24 h) did not detectably impair epithelium morphology (Figure 3C) and Ecad luminal accessibility compared to WT organoids (Figures 4B and S2; Video S5).

Microinjection experiments revealed that induction of Rab7DN did not affect bacterial translocation through goblet cells. *Listeria* was found extracellular at the basolateral pole of goblet cells of Rab7DN-induced organoids, to the same degree as in transduced but non-induced control organoids (NI). This shows that bacteria complete translocation normally within goblet cells in presence of Rab7DN (Figures 4C–4E, Rab7DN, and S3; Video S5). In contrast, in mycRab11DN-induced transduced organoids, a significant decrease of translocated bacteria beneath goblet cells was observed, together with a corresponding significant increase of intracellular bacteria. Intracellular bacteria were mostly located at the basolateral pole of goblet cells (Figures 4C–4E, Rab11DN, and S3; Video S5). This was also the case for wild-type *Listeria* microinjected in mycRab11DN-induced organoids, even 16 h post-microinjection (Figures S2D–S2F). Note that prolonged exposure to doxycycline might have prevented *Listeria* vacuolar escape and cell-to-cell spread at this late time point. Taken together, these data show that Rab11, in contrast to Rab7, is required for the release of bacteria from the basal pole of goblet cells, highlighting that *Listeria* hijacks Rab11-dependent Ecad recycling for trans-epithelial translocation via goblet cells.

Organoid as a Model for Real-Time Investigations of Host-Pathogen Interactions

Here, we have developed an *ex vivo* minigut system in which *Listeria* crosses the intestinal barrier by transcytosis through goblet cells as it does *in vivo*.⁶ We have harnessed the power of this experimental system to directly image, in real time, the trans-epithelial translocation of a microbial pathogen and to dissect the underlying cell biology and molecular mechanisms. *Listeria* crossing of the intestinal barrier relies on the specific interaction of InIA with lumenally accessible Ecad at the apical pole of goblet cells. We have shown that (1) bacterial Ecad-dependent internalization in goblet cells requires dynamin-mediated endocytosis, (2) bacteria transit through these cells in a microtubule-dependent manner as *in vivo*,⁶ and (3) Rab11 is required for the release of *Listeria* at the basolateral pole of goblet cells, thereby showing that *Listeria* hijacks E-cadherin recycling pathway to cross the intestinal barrier (Figure S3). Although organoids have been used to investigate infection with human norovirus and SARS-CoV-2^{45,46} and the interactions of enteropathogens, such as *Salmonella enterica*⁴⁷ and *Cryptosporidium parvum* with the intestinal epithelium,⁴⁸ here, we have microinjected for the first time microbes in the lumen of

Figure 3. Inducible Organoids Expressing Dominant-Negative Rab11 and Rab7

(A) Scheme depicting the organoid transduction.
(B) Visualization of successful induction with Dox for 16 h. mCerulean (mCer) expression was detected by eyes using Zeiss Filter set 38 high efficiency (HE) excitation band pass (BP) 470/40; beamsplitter farbteiler (FT) 495; emission BP 525/50.
(C) Confocal imaging of permeabilized, whole-mount stained organoids induced with indicated DN proteins for 16 h with Dox. Expression of DN proteins is visualized by anti-Rab7 (Rab7DN) or anti-myc (Rab11DN) staining. In mycRab11DN-induced organoids, mCer co-localized with myc staining (not shown). Goblet-cell-producing mucus is labeled with WGA (arrow). Junctional integrity of organoids is evaluated by Ecad staining.

intestinal organoids, imaged in real time microbial crossing of the intestinal barrier, and deciphered the underlying molecular mechanisms of microbial translocation. This novel *ex vivo* system of infection opens a wide range of opportunities to study pathogen interactions with host barriers in a direct manner, in contrast to what has been done so far. Additionally, this study also pioneers the use of genetically modified inducible organoids to address the cellular and molecular mechanisms of host-pathogen interactions in a tissue context. Rab11 has been shown to be necessary for Ecad recycling in mammalian cells and *in vivo* in *Drosophila melanogaster*.⁸ Moreover, Rab11 is required for basolateral trafficking of newly synthesized Ecad in polarized Madin-Darby Canine Kidney (MDCK) cells.³⁸ However, the cellular trafficking of Ecad from its apical to basolateral pole from either side of adherens junctions had not been thoroughly investigated in a tissue context to our knowledge. It has been previously shown in non-polarized epithelial intestinal Caco-2 and trophoblastic JEG3 cell lines that, upon binding of InIA to Ecad, the plasma membrane is remodeled in an actin-dependent manner and leads to caveolin- and clathrin-dependent bacterial endocytosis.^{32,49–53} In cultured epithelial cells, *Listeria* internalization occurs mainly at the edge of cell islets, where cells are non-polarized and Ecad is broadly accessible. Once internalized into these non-polarized cells, *Lm* escapes from the vacuole in an LLO-dependent manner and propels itself through ActA in the cytosol.⁵⁴ Here, we have shown that, in polarized differentiated goblet cells in a tissue context, the initial step of internalization through accessible Ecad is also dynamin dependent. However, after completing bacterial internalization, *Lm* is rapidly transferred and released to the basolateral pole of goblet cells, owing to the rapid Rab11-dependent recycling of Ecad. This may protect invading bacteria from epithelial innate immune responses and favor their dissemination in host tissues. Live imaging of host-pathogen interactions in organoids is a promising approach to dissect their underlying cell and molecular biology.

STAR★METHODS

Detailed methods are provided in the online version of this paper and include the following:

- KEY RESOURCES TABLE
- RESOURCE AVAILABILITY
 - Lead Contact
 - Materials Availability
 - Data and Code Availability

● EXPERIMENTAL MODEL AND SUBJECT DETAILS

- Bacteria
- Mice
- Organoids
- Cells

● METHOD DETAILS

- Organoid microinjection
- Accessible Ecad detection
- Immunofluorescence
- Imaging
- Rab11DN and Rab7DN vector construction
- Lentivirus production and concentration
- Organoid transduction

● QUANTIFICATION AND STATISTICAL ANALYSIS

- Statistical Analysis

SUPPLEMENTAL INFORMATION

Supplemental Information can be found online at <https://doi.org/10.1016/j.cub.2020.11.041>.

ACKNOWLEDGMENTS

We thank Dr. Thaddeus Stappenbeck, Washington University in Saint Louis, USA, and Corinne Lebreton, Institut Imagine, Paris, France, for the L-WRN cell line. We thank Miranda Vogt, Stanford University, USA, for her contribution to this study as a summer student. We thank Image Analysis Hub of the Institut Pasteur for the help and the members of Biology of Infection Unit for their support. M.K. received a long-term postdoctoral fellowship from the European Molecular Biology Organization (EMBO), ALTF 1192-2017. Institut Pasteur, Inserm, LabEx IBEID, the European Research Council (ERC) Invadis, and ANR Organolist provided financial support.

AUTHOR CONTRIBUTIONS

M. Lecuit conceived the project, designed the study, directed the research, participated in the analysis of the data, and edited the manuscript. M.K. designed and performed experiments, analyzed data, and wrote the manuscript. C.F. designed and performed some experiments and analyzed some of the data. M. Lavina provided technical help. O.D. participated in the supervision of the study, data analysis, and writing and editing of the manuscript.

DECLARATION OF INTERESTS

The authors declare no competing interests.

Received: July 1, 2020
Revised: October 13, 2020
Accepted: November 17, 2020
Published: December 16, 2020

FT 495; emission BP 525/50; Figure 3B). Induced organoids were selected and microinjected, incubated for 2 h (DN proteins still being induced), and followed by fixation and imaging.

(B) Luminally accessible Ecad of the sectioned organoids induced with indicated DN proteins. Accessible Ecad staining in XY, XZ, and YZ planes from indicated goblet cells is shown (arrow from the right 3D reconstruction; sectioned plane facing up in the side view). See also Video S5.

(C) Optical sections from 3D reconstruction of microinjected organoids induced for indicated DN proteins. *Li*-GFP (InIA) can be detected beneath the basolateral side of the goblet cells in transduced but non-induced control (top) and in Rab7DN-induced organoids (center), indicating that bacterial translocation occurred. *Li*-GFP (InIA) is trapped at the basal pole of the goblet cell, embedded in WGA⁺ material in mycRab11DN-induced organoids (bottom). Goblet cells are marked with an arrow. Scale bars, 20 μ m. See also Figure S3 and Video S5.

(D) Quantification of number of cells associated with bacteria per organoids. Kruskal-Wallis test; comparison to WT; NI, Lentivirus transduced, non-induced control.

(E) Quantification of number of bacteria per organoid in indicated location. Experiments were repeated 2 to 3 times. The results combine all experiments. Counts were performed in 19 non-induced, 18 Rab7DN, and 24 Rab11DN organoids. The results for WT organoids are those from Figures 2B and 2C. Kruskal-Wallis test; comparison to WT; * $p < 0.05$; ** $p < 0.01$. See also Figure S3.

REFERENCES

- Lecuit, M. (2020). *Listeria monocytogenes*, a model in infection biology. *Cell. Microbiol.* 22, e13186.
- Gaillard, J.L., Berche, P., Frehel, C., Gouin, E., and Cossart, P. (1991). Entry of *L. monocytogenes* into cells is mediated by internalin, a repeat protein reminiscent of surface antigens from gram-positive cocci. *Cell* 65, 1127–1141.
- Mengaud, J., Ohayon, H., Gounon, P., Mege R-M, and Cossart, P. (1996). E-cadherin is the receptor for internalin, a surface protein required for entry of *L. monocytogenes* into epithelial cells. *Cell* 84, 923–932.
- Lecuit, M., Dramsi, S., Gottardi, C., Fedor-Chaiken, M., Gumbiner, B., and Cossart, P. (1999). A single amino acid in E-cadherin responsible for host specificity towards the human pathogen *Listeria monocytogenes*. *EMBO J.* 18, 3956–3963.
- Lecuit, M., Vandormael-Pourmin, S., Lefort, J., Huerre, M., Gounon, P., Dupuy, C., Babinet, C., and Cossart, P. (2001). A transgenic model for listeriosis: role of internalin in crossing the intestinal barrier. *Science* 292, 1722–1725.
- Nikitas, G., Deschamps, C., Disson, O., Niaux, T., Cossart, P., and Lecuit, M. (2011). Transcytosis of *Listeria monocytogenes* across the intestinal barrier upon specific targeting of goblet cell accessible E-cadherin. *J. Exp. Med.* 208, 2263–2277.
- Le, T.L., Yap, A.S., and Stow, J.L. (1999). Recycling of E-cadherin: a potential mechanism for regulating cadherin dynamics. *J. Cell Biol.* 146, 219–232.
- Brüser, L., and Bogdan, S. (2017). Adherens junctions on the move—membrane trafficking of E-cadherin. *Cold Spring Harb. Perspect. Biol.* 9, a029140.
- Sato, T., Vries, R.G., Snippert, H.J., van de Wetering, M., Barker, N., Stange, D.E., van Es, J.H., Abo, A., Kujala, P., Peters, P.J., and Clevers, H. (2009). Single Lgr5 stem cells build crypt-villus structures in vitro without a mesenchymal niche. *Nature* 459, 262–265.
- Koo, B.K., Stange, D.E., Sato, T., Karthaus, W., Farin, H.F., Huch, M., van Es, J.H., and Clevers, H. (2011). Controlled gene expression in primary Lgr5 organoid cultures. *Nat. Methods* 9, 81–83.
- Maru, Y., Orihashi, K., and Hippo, Y. (2016). Lentivirus-based stable gene delivery into intestinal organoids. *Methods Mol. Biol.* 1422, 13–21.
- Van Lidth de Jeude, J.F., Vermeulen, J.L., Montenegro-Miranda, P.S., Van den Brink, G.R., and Heijmans, J. (2015). A protocol for lentiviral transduction and downstream analysis of intestinal organoids. *J. Vis. Exp.* 52531.
- Schwank, G., and Clevers, H. (2016). CRISPR/Cas9-mediated genome editing of mouse small intestinal organoids. *Methods Mol. Biol.* 1422, 3–11.
- Yin, X., Farin, H.F., van Es, J.H., Clevers, H., Langer, R., and Karp, J.M. (2014). Niche-independent high-purity cultures of Lgr5+ intestinal stem cells and their progeny. *Nat. Methods* 11, 106–112.
- McKinley, K.L., Stuurman, N., Royer, L.A., Scharfner, C., Castillo-Azofeifa, D., Delling, M., Klein, O.D., and Vale, R.D. (2018). Cellular aspect ratio and cell division mechanics underlie the patterning of cell progeny in diverse mammalian epithelia. *eLife* 7, e36739.
- Disson, O., Grayo, S., Huillet, E., Nikitas, G., Langa-Vives, F., Dussurget, O., Ragon, M., Le Monnier, A., Babinet, C., Cossart, P., and Lecuit, M. (2008). Conjugated action of two species-specific invasion proteins for fetoplacental listeriosis. *Nature* 455, 1114–1118.
- de Lau, W., Kujala, P., Schneeberger, K., Middendorp, S., Li, V.S., Barker, N., Martens, A., Hoffhuis, F., DeKoter, R.P., Peters, P.J., et al. (2012). Peyer's patch M cells derived from Lgr5(+) stem cells require SpiB and are induced by RankL in cultured "miniguts". *Mol. Cell. Biol.* 32, 3639–3647.
- Colony, P.C. (1996). Structural characterization of colonic cell types and correlation with specific functions. *Dig. Dis. Sci.* 41, 88–104.
- Johansson, M.E., and Hansson, G.C. (2012). Preservation of mucus in histological sections, immunostaining of mucins in fixed tissue, and localization of bacteria with FISH. *Methods Mol. Biol.* 842, 229–235.
- Fischer, J., Uhlenbruck, G., Klein, P.J., Vierbuchen, M., and Fischer, R. (1984). Characterization of glycoconjugates of human gastrointestinal mucosa by lectins. II. Lectin binding to the isolated glycoproteins of normal and malignant gastric mucosa. *J. Histochem. Cytochem.* 32, 690–696.
- Fischer, J., Klein, P.J., Vierbuchen, M., Skutta, B., Uhlenbruck, G., and Fischer, R. (1984). Characterization of glycoconjugates of human gastrointestinal mucosa by lectins. I. Histochemical distribution of lectin binding sites in normal alimentary tract as well as in benign and malignant gastric neoplasms. *J. Histochem. Cytochem.* 32, 681–689.
- Knoop, K.A., McDonald, K.G., McCrate, S., McDole, J.R., and Newberry, R.D. (2015). Microbial sensing by goblet cells controls immune surveillance of luminal antigens in the colon. *Mucosal Immunol.* 8, 198–210.
- Lecuit, M., Ohayon, H., Braun, L., Mengaud, J., and Cossart, P. (1997). Internalin of *Listeria monocytogenes* with an intact leucine-rich repeat region is sufficient to promote internalization. *Infect. Immun.* 65, 5309–5319.
- Coelho, C., Brown, L., Maryam, M., Vij, R., Smith, D.F.Q., Burnet, M.C., Kyle, J.E., Heyman, H.M., Ramirez, J., Prados-Rosales, R., et al. (2019). *Listeria monocytogenes* virulence factors, including listeriolysin O, are secreted in biologically active extracellular vesicles. *J. Biol. Chem.* 294, 1202–1217.
- Hunt, S.D., Townley, A.K., Danson, C.M., Cullen, P.J., and Stephens, D.J. (2013). Microtubule motors mediate endosomal sorting by maintaining functional domain organization. *J. Cell Sci.* 126, 2493–2501.
- Desclozeaux, M., Venturato, J., Wylie, F.G., Kay, J.G., Joseph, S.R., Le, H.T., and Stow, J.L. (2008). Active Rab11 and functional recycling endosome are required for E-cadherin trafficking and lumen formation during epithelial morphogenesis. *Am. J. Physiol. Cell Physiol.* 295, C545–C556.
- Langevin, J., Morgan, M.J., Sibarita, J.-B., Aresta, S., Murthy, M., Schwarz, T., Camonis, J., and Bellaïche, Y. (2005). *Drosophila* exocyst components Sec5, Sec6, and Sec15 regulate DE-Cadherin trafficking from recycling endosomes to the plasma membrane. *Dev. Cell* 9, 365–376.
- Palacios, F., Schweitzer, J.K., Boshans, R.L., and D'Souza-Schorey, C. (2002). ARF6-GTP recruits Nm23-H1 to facilitate dynamin-mediated endocytosis during adherens junctions disassembly. *Nat. Cell Biol.* 4, 929–936.
- de Beco, S., Gueudry, C., Amblard, F., and Coscoy, S. (2009). Endocytosis is required for E-cadherin redistribution at mature adherens junctions. *Proc. Natl. Acad. Sci. USA* 106, 7010–7015.
- Delevoeye, C., Miserey-Lenkei, S., Montagnac, G., Gilles-Marsens, F., Paul-Gilloteaux, P., Giordano, F., Waharte, F., Marks, M.S., Goud, B., and Raposo, G. (2014). Recycling endosome tubule morphogenesis from sorting endosomes requires the kinesin motor KIF13A. *Cell Rep.* 6, 445–454.
- Meng, W., Mushika, Y., Ichii, T., and Takeichi, M. (2008). Anchorage of microtubule minus ends to adherens junctions regulates epithelial cell-cell contacts. *Cell* 135, 948–959.
- Veiga, E., Guttman, J.A., Bonazzi, M., Boucrot, E., Toledo-Arana, A., Lin, A.E., Enninga, J., Pizarro-Cerdá, J., Finlay, B.B., Kirchhausen, T., and Cossart, P. (2007). Invasive and adherent bacterial pathogens co-opt host clathrin for infection. *Cell Host Microbe* 2, 340–351.
- Macia, E., Ehrlich, M., Massol, R., Boucrot, E., Brunner, C., and Kirchhausen, T. (2006). Dynasore, a cell-permeable inhibitor of dynamin. *Dev. Cell* 10, 839–850.
- Taylor, E.W. (1965). The mechanism of colchicine inhibition of mitosis. I. Kinetics of inhibition and the binding of H₃-colchicine. *J. Cell Biol.* 25 (SUPPL), 145–160.
- Kessell, I., Holst, B.D., and Roth, T.F. (1989). Membranous intermediates in endocytosis are labile, as shown in a temperature-sensitive mutant. *Proc. Natl. Acad. Sci. USA* 86, 4968–4972.

36. Damke, H., Baba, T., Warnock, D.E., and Schmid, S.L. (1994). Induction of mutant dynamin specifically blocks endocytic coated vesicle formation. *J. Cell Biol.* *127*, 915–934.
37. Henley, J.R., Krueger, E.W., Oswald, B.J., and McNiven, M.A. (1998). Dynamins mediate internalization of caveolae. *J. Cell Biol.* *141*, 85–99.
38. Lock, J.G., and Stow, J.L. (2005). Rab11 in recycling endosomes regulates the sorting and basolateral transport of E-cadherin. *Mol. Biol. Cell* *16*, 1744–1755.
39. Woichansky, I., Beretta, C.A., Berns, N., and Riechmann, V. (2016). Three mechanisms control E-cadherin localization to the zonula adherens. *Nat. Commun.* *7*, 10834.
40. Sönnichsen, B., De Renzis, S., Nielsen, E., Rietdorf, J., and Zerial, M. (2000). Distinct membrane domains on endosomes in the recycling pathway visualized by multicolor imaging of Rab4, Rab5, and Rab11. *J. Cell Biol.* *149*, 901–914.
41. Ullrich, O., Reinsch, S., Urbé, S., Zerial, M., and Parton, R.G. (1996). Rab11 regulates recycling through the pericentriolar recycling endosome. *J. Cell Biol.* *135*, 913–924.
42. Yu, S., Yehia, G., Wang, J., Stypulkowski, E., Sakamori, R., Jiang, P., Hernandez-Enriquez, B., Tran, T.S., Bonder, E.M., Guo, W., and Gao, N. (2014). Global ablation of the mouse Rab11a gene impairs early embryogenesis and matrix metalloproteinase secretion. *J. Biol. Chem.* *289*, 32030–32043.
43. Sobajima, T., Yoshimura, S., Iwano, T., Kunii, M., Watanabe, M., Atik, N., Mushiaki, S., Morii, E., Koyama, Y., Miyoshi, E., and Harada, A. (2014). Rab11a is required for apical protein localisation in the intestine. *Biol. Open* *4*, 86–94.
44. Palacios, F., Tushir, J.S., Fujita, Y., and D'Souza-Schorey, C. (2005). Lysosomal targeting of E-cadherin: a unique mechanism for the down-regulation of cell-cell adhesion during epithelial to mesenchymal transitions. *Mol. Cell. Biol.* *25*, 389–402.
45. Ettayebi, K., Crawford, S.E., Murakami, K., Broughman, J.R., Karandikar, U., Tenge, V.R., Neill, F.H., Blatt, S.E., Zeng, X.L., Qu, L., et al. (2016). Replication of human noroviruses in stem cell-derived human enteroids. *Science* *353*, 1387–1393.
46. Lamers, M.M., Beumer, J., van der Vaart, J., Knoops, K., Puschhof, J., Breugem, T.I., Ravelli, R.B.G., Paul van Schayck, J., Mykytyn, A.Z., Duimel, H.Q., et al. (2020). SARS-CoV-2 productively infects human gut enterocytes. *Science* *369*, 50–54.
47. Forbester, J.L., Goulding, D., Vallier, L., Hannan, N., Hale, C., Pickard, D., Mukhopadhyay, S., and Dougan, G. (2015). Interaction of *Salmonella enterica* serovar typhimurium with intestinal organoids derived from human induced pluripotent stem cells. *Infect. Immun.* *83*, 2926–2934.
48. Heo, I., Dutta, D., Schaefer, D.A., Iakobachvili, N., Artegiani, B., Sachs, N., Boonekamp, K.E., Bowden, G., Hendrickx, A.P.A., Willems, R.J.L., et al. (2018). Modelling *Cryptosporidium* infection in human small intestinal and lung organoids. *Nat. Microbiol.* *3*, 814–823.
49. Lecuit, M., Hurme, R., Pizarro-Cerda, J., Ohayon, H., Geiger, B., and Cossart, P. (2000). A role for alpha- and beta-catenins in bacterial uptake. *Proc. Natl. Acad. Sci. USA* *97*, 10008–10013.
50. Bonazzi, M., Veiga, E., Pizarro-Cerdá, J., and Cossart, P. (2008). Successive post-translational modifications of E-cadherin are required for InlA-mediated internalization of *Listeria monocytogenes*. *Cell. Microbiol.* *10*, 2208–2222.
51. Sousa, S., Cabanes, D., El-Amraoui, A., Petit, C., Lecuit, M., and Cossart, P. (2004). Unconventional myosin VIIa and vezatin, two proteins crucial for *Listeria* entry into epithelial cells. *J. Cell Sci.* *117*, 2121–2130.
52. Sousa, S., Cabanes, D., Bougnères, L., Lecuit, M., Sansonetti, P., Tran-Van-Nhieu, G., and Cossart, P. (2007). Src, cortactin and Arp2/3 complex are required for E-cadherin-mediated internalization of *Listeria* into cells. *Cell. Microbiol.* *9*, 2629–2643.
53. Sousa, S., Cabanes, D., Archambaud, C., Colland, F., Lemichez, E., Popoff, M., Boisson-Dupuis, S., Gouin, E., Lecuit, M., Legrain, P., and Cossart, P. (2005). ARHGAP10 is necessary for alpha-catenin recruitment at adherens junctions and for *Listeria* invasion. *Nat. Cell Biol.* *7*, 954–960.
54. Tilney, L.G., and Portnoy, D.A. (1989). Actin filaments and the growth, movement, and spread of the intracellular bacterial parasite, *Listeria monocytogenes*. *J. Cell Biol.* *109*, 1597–1608.
55. Dramsi, S., Lévi, S., Triller, A., and Cossart, P. (1998). Entry of *Listeria monocytogenes* into neurons occurs by cell-to-cell spread: an in vitro study. *Infect. Immun.* *66*, 4461–4468.
56. Dramsi, S., Biswas, I., Maguin, E., Braun, L., Mastroeni, P., and Cossart, P. (1995). Entry of *Listeria monocytogenes* into hepatocytes requires expression of inlB, a surface protein of the internalin multigene family. *Mol. Microbiol.* *16*, 251–261.
57. Levraud, J.P., Disson, O., Kissa, K., Bonne, I., Cossart, P., Herbomel, P., and Lecuit, M. (2009). Real-time observation of *Listeria monocytogenes*-phagocyte interactions in living zebrafish larvae. *Infect. Immun.* *77*, 3651–3660.
58. Balestrino, D., Hamon, M.A., Dortet, L., Nahori, M.A., Pizarro-Cerda, J., Alignani, D., Dussurget, O., Cossart, P., and Toledo-Arana, A. (2010). Single-cell techniques using chromosomally tagged fluorescent bacteria to study *Listeria monocytogenes* infection processes. *Appl. Environ. Microbiol.* *76*, 3625–3636.
59. Muzumdar, M.D., Tasic, B., Miyamichi, K., Li, L., and Luo, L. (2007). A global double-fluorescent Cre reporter mouse. *Genesis* *45*, 593–605.
60. Mahe, M.M., Aihara, E., Schumacher, M.A., Zavros, Y., Montrose, M.H., Helmrich, M.A., Sato, T., and Shroyer, N.F. (2013). Establishment of gastrointestinal epithelial organoids. *Curr. Protoc. Mouse Biol.* *3*, 217–240.
61. Waddell, A., Vallance, J.E., Hummel, A., Alenghat, T., and Rosen, M.J. (2019). IL-33 induces murine intestinal goblet cell differentiation indirectly via innate lymphoid cell IL-13 secretion. *J. Immunol.* *202*, 598–607.
62. Wu, D., Ahrens, R., Osterfeld, H., Noah, T.K., Groschwitz, K., Foster, P.S., Steinbrecher, K.A., Rothenberg, M.E., Shroyer, N.F., Matthaei, K.I., et al. (2011). Interleukin-13 (IL-13)/IL-13 receptor alpha1 (IL-13Ralpha1) signaling regulates intestinal epithelial cystic fibrosis transmembrane conductance regulator channel-dependent Cl⁻ secretion. *J. Biol. Chem.* *286*, 13357–13369.
63. van Es, J.H., van Gijn, M.E., Riccio, O., van den Born, M., Vooijs, M., Begthel, H., Cozijnsen, M., Robine, S., Winton, D.J., Radtke, F., and Clevers, H. (2005). Notch/gamma-secretase inhibition turns proliferative cells in intestinal crypts and adenomas into goblet cells. *Nature* *435*, 959–963.
64. Nigro, G., Hanson, M., Fevre, C., Lecuit, M., and Sansonetti, P.J. (2019). Intestinal organoids as a novel tool to study microbes-epithelium interactions. *Methods Mol. Biol.* *1576*, 183–194.
65. Johansson, M.E., Phillipson, M., Petersson, J., Velcich, A., Holm, L., and Hansson, G.C. (2008). The inner of the two Muc2 mucin-dependent mucus layers in colon is devoid of bacteria. *Proc. Natl. Acad. Sci. USA* *105*, 15064–15069.

STAR★METHODS

KEY RESOURCES TABLE

REAGENT or RESOURCE	SOURCE	IDENTIFIER
Antibodies and fluorescent dyes		
Rat anti-E-cad (ECCD-2)	Takara	#M108
Rabbit anti Rab7	Sigma	R4779; RRID:AB_477460
Rabbit antisera against <i>Listeria monocytogenes</i>	55	R11
Mouse IgG1 anti-myc (71D10)	Cell signaling	#2278; RRID:AB_490778
WGA-conjugated with Alexa Fluor 647	Invitrogen	W32466
Hoechst 33342	Invitrogen	H3570
Goat anti-Rat Alexa Fluor 546	Invitrogen	#A-11081; RRID:AB_141738
Goat anti-Rabbit Alexa Fluor 405	Invitrogen	#A-31556; RRID:AB_221605
Goat anti-Mouse Alexa Fluor 405	Invitrogen	#A-31553; RRID:AB_221604
Bacterial and Virus Strains		
<i>Lm</i> strain EGD	56	BUG600
EGD Δ <i>inlA</i>	56	BUG 947
EGD Δ <i>hly</i>	57	BUG 2132
EGD Δ <i>actA</i>	57	BUG 2140
<i>Li</i> WT	55	BUG 499
<i>Li</i> (InlA+)	23	BUG 1489
<i>Li</i> -GFP (InlA+)	This paper	MBHL 366
rLV.EF1.Tet3G-9	Takara	631311
Chemicals, Peptides, and Recombinant Proteins		
N2 Supplement	GIBCO Invitrogen	#17502048
B27 Supplement	GIBCO Invitrogen	#17504044
N-Acetylcystein	Sigma Aldrich	#A9165-5G
Human recombinant R-spondin 1 (final 500 ng/ml)	R&D systems	#4645-RS250
Mouse recombinant Noggin (final 100 ng/ml)	Peptotech	#250-38-20ug
Mouse recombinant EGF (final 50 ng/ml)	Invitrogen	#PMG8044
Y-27632 (final 10 uM)	Sigma Aldrich	#Y0503-1MG
Mouse recombinant Wnt3a (final 100 ng/ml)	Millipore	#GF160
Nicotinamide (final 10 mM)	Sigma Aldrich	#N0636-100 g
CHIR99021 (final 10 uM)	Stemgent	#248040004
Doxycycline (final 2 ug/ml)	Takara	#631311
Dynasore (final 80 uM)	Sigma	324410-10MG
Colchicine (final 10 ug/ml)	Sigma	C3915
DATP (final 10 uM)	Stemgent	#04-0041
IL-13 (final 20 ng/ml)	R&D systems	#413-ML-005
TransDux MAX™	System Bioscience	LV860A-1
Matrigel	Corning	356231
Cell recovery solution	BD	354253
Advanced DMEM/F12	GIBCO Invitrogen	12634010
DMEM/F12 phenol red-free	GIBCO Invitrogen	21041025
GlutaMAX	GIBCO Invitrogen	35050038
1M HEPES	GIBCO Invitrogen	15630056
Penicillin-streptomycin	GIBCO Invitrogen	15140163
Puromycin (final 1 ug/ml)	Sigma	540411-25MG
Neomycin (Geneticin, final 1X)	GIBCO Invitrogen	10138031

(Continued on next page)

Continued		
REAGENT or RESOURCE	SOURCE	IDENTIFIER
Critical Commercial Assays		
Calcium phosphate transfection kit	Takara	#631312
PEG-it™ Virus precipitation solution	System Bioscience	# LV810A-1
Experimental Models: Cell Lines		
HEK293T	ATCC	#CRL-11268
L-WRN	ATCC	#CRL-3276
Experimental Models: Organisms/Strains		
Mouse (KI E16P) intestinal organoid	This paper and ¹⁶	N/A
Mouse (mtd-Tmt; KI E16P) intestinal organoid	This paper and ⁶	N/A
Oligonucleotides		
Primer for Rab11DN 5'-GTGTTGGAAAGAACAACCTCCTGTCTCGATTTA-3'	This paper	N/A
Primer for Rab11DN 5'-GACAGGAGGTTGTTCTTTCCAACACCAGAATC-3'	This paper	N/A
Primer for Rab7DN 5'-CTGGTGTGGAAAGAAGCTCTCTCATGAACCAG -3'	This paper	N/A
Primer for Rab7DN 5'-CTGGTTCATGAGAGAGTTCTTTCCAACACCAG -3'	This paper	N/A
Recombinant DNA		
pAD	⁵⁸	N/A
psPAX2	Addgene	#12260
pMD2.G	Addgene	#12259
pTREG3-IRES	Takara	#631312
pCMV-intron-mycRab11	Addgene	#46785
pCMV-SPORT6-Rab7	Addgene and this paper	N/A
Software and Algorithms		
Prism 8	Graphpad	N/A
Arivis Vision4D 3.0.	Arivis	N/A
Fiji	ImageJ	N/A
ZEN 2014 SP1	ZEISS	N/A

RESOURCE AVAILABILITY

Lead Contact

Further information and requests for resources and reagents should be directed to and will be fulfilled by the Lead Contact, Marc Lecuit (marc.lecuit@pasteur.fr).

Materials Availability

All plasmids generated in this study are available upon request.

Data and Code Availability

This study did not generate/analyze datasets or codes

EXPERIMENTAL MODEL AND SUBJECT DETAILS

Bacteria

For Figures 1B and 1C, *Lm* strain EGD (BUG 600) and isogenic deletion mutants Δ *lnIA* (BUG 947⁵⁶), Δ *hly* (BUG 2132⁵⁷), Δ *actA* (BUG 2140⁵⁷), *Li* WT (BUG 499), *Li*-expressing *lnIA* (*Li* (*lnIA*+), BUG 1489²³) were used. We generated *Li*-expressing both *lnIA* and GFP in tandem under the phyper promoter of pAD vector, separated by the terminator sequence (MBHL 366). Bacteria were transformed by electroporation. GFP expression was confirmed by fluorescent microscopy, function of *lnIA* was confirmed by *in vitro* invasion assay using mouse fibroblast L2071 expressing human E-cadherin⁴⁹.

Mice

E16P KI mice were generated in the laboratory¹⁶. They were crossed with mT/mG mice⁵⁹ to generate mtd-Tmt; E16P KI mice. Animal experiments were performed according to the Institut Pasteur guidelines for laboratory animals' husbandry and in compliance with

European regulation 2010/63 EU. They were approved by the ethical committee CETEA/CEEA No. 89 of Institut Pasteur under the number DHA180011.

Organoids

Intestinal organoids were generated and cultured from the crypts recovered from small intestines of 6- to 8-week old KIE16P and mtd-Tmt; E16P KI mice using EDTA dissociation method^{9,60}. They were grown in ENR medium (Advanced DMEM/F12 with EGF (50 ng/ml), Noggin (100 ng/ml) and R-spondin1 (500 ng/ml)).

Cells

HEK293T cells (ATCC CRL-11268) were grown and passaged in DMEM containing 2% glutamine, 10% Tet-system approved FBS (Takara # 631106) and penicillin-streptomycin.

METHOD DETAILS

Organoid microinjection

Mature organoids growing in ENR medium were mechanically dissociated and passed into the gridded, low-bottom iBidi-injection plate (Clinisciences # 80156). Result of Figures 1B and 1C was obtained with ENR medium while all others were obtained using the following condition: Organoids were passed in injection plates with 2:1 ratio of ENR and 50% of L-WRN cell-conditioned media (made with Tet System Approved FBS, Takara # 631106) for 1-2 days to have a round center to facilitate microinjection. When the organoids produced spherical centers, the organoids were washed several times with pre-warmed Advanced DMEM/F12 to remove the serum and excessive growth factors, replaced with either ENR or 5% L-WRN conditioned media for minimal 1 day. A day before the microinjection, 10 μ M DAPT and 20 μ g/ml IL-13 were supplemented overnight to partially enrich the goblet cells and to induce mucus expel from the existing goblet cells⁶¹⁻⁶³. Figure 2A, final concentration of 80 μ M dynasore or 10 μ g/ml colchicine were applied 2 hours prior to microinjection. Figures 4A and 4C, final concentration of 2 μ g/ml doxycycline was added to the media 12-16 hours before the microinjection. Microinjection was performed only to organoids verified to have successful induction. Results of Figures 1B and 1C were obtained by fixing 1 hour and 16 hours, respectively, after microinjection. The incubation period post microinjection of the other experiments was optimized to 2 hours followed by fixation to reduce the damage of the organoids. Drug/doxycycline treatment was maintained during this period. For live imaging, immediately after microinjection, organoids were re-sampled to the imaging chamber of light sheet microscope Zeiss Z1.

Overnight culture of bacteria was diluted (1/200) and grown until O.D 0.8, washed at least 3 times in PBS and collected as a final volume of 100 μ l in DMEM/F12 phenol red-free medium. Microinjection was performed with Eppendorf InjectMan and FemtoJet system as reported⁶⁴ using glass micropipettes injection needle (Vitromed # V-INJ-S3-35).

Accessible Ecad detection

Organoids were passed on the 8-well Lab-Tek plates and supplied with the media as for the microinjection: first with 2:1 ratio of ENR and 50% L-WRN cell conditioned media to grow the spherical center, followed by washing and either returned to ENR media or supplied with 5% L-WRN media for at least 1 day. A day before the fixation, organoids were treated at a final concentration of 10 μ M DAPT and 20 ng/ml IL-13 overnight to induce mucus expel from the existing goblet cells. Organoids were fixed with 4% PFA at 4°C overnight. For the experiments in Figure 2D, final concentration of 80 μ M dynasore or 10 μ g/ml colchicine were added 2 hours before fixation. Experiment of Figure 4B, final concentration of 2 μ g/ml doxycycline was added 12-16 hours before fixation. When the organoids were fixed, PFA was removed, organoids were washed and 6% low-melting agarose was poured to the wells. Solidified wells were recovered, sectioned in 150-200 μ m thickness with a vibratome (Micro HM 650V, Thermo Fisher Scientific). Sections containing opened organoids were blocked in 3% BSA in PBS and stained as indicated below.

Immunofluorescence

Accessible Ecad (Figures 1E, 2C, and 4B): Organoids were fixed with 4% PFA at 4°C overnight followed by washing and blocking with 3% BSA in PBS, overnight at room temperature. Primary and secondary antibodies were applied for 1 hour at room temperature.

Whole-mount staining: Organoids were fixed with 4% PFA for 30 min – 1 hour at room temperature followed by washing, blocking/permeabilizing for 2 hours either in 5% goat serum with 1% Triton X-100 or in 3% BSA with 1% Triton X-100 in PBS. Primary antibodies were applied at 4°C overnight followed by washing and stained with secondary antibodies for 2 hours at room temperature or 4°C overnight.

Distinguishing intracellular versus translocated bacteria (Figure 1B): Organoids were fixed with 4% PFA at 37°C for 1 hour, washed and blocked without triton for 2 hours at room temperature. Rabbit antisera against *Listeria monocytogenes* (R11⁵⁵) was added for 2 hours at room temperature, followed by washing and secondary antibody for 1 hour at room temperature to stain extra-organoid bacteria. Then microinjected organoids were permeabilized with 1% Triton X-100 and stained with primary antibody at 4°C overnight followed by washing and secondary antibody for 2 hours at room temperature.

The following antibodies were used: anti-Ecad (Eccd2, Takara #M108, 1:350), anti-myc (71D10, Cell Signaling # 2278, 1:500), anti-Rab7 (Sigma, #R4779, 1:200), WGA conjugated with alexa 647 (Invitrogen, whole mount 1:300, section 1:1000) and Hoechst 33342 (Invitrogen 1:5000). Secondary antibodies include goat anti-rat conjugated with alexa 546, goat anti-mouse conjugated with alexa

405, and goat anti-rabbit conjugated with alexa 405 (all Invitrogen 1:500). To identify the goblet cells, the following criteria were used, as the Muc2 labeling method following Carnoy fixation and paraffin embedding⁶⁵ is not compatible with our system, rendering the matrigel opaque as well as breaking the plate: WGA⁺, typical goblet-shaped cellular morphology including the opening of the apical area and the nucleus misaligned with neighboring cells. If the cells meet 2 or more conditions, we regarded them as goblet cells.

Imaging

Images were acquired either by confocal microscope (fixed image, upright Zeiss LSM 700 equipped with a water Plan-Apochromat 40x/1.0 DIC M27 objective & inverted Zeiss LSM 710 equipped with an oil Plan-Apochromat 40x/1.3 DIC M27 objective) or light sheet microscope (live image, Zeiss Z.1 equipped with a water Plan-Apochromat 40x/1.0 DIC objective). For live imaging, imaging chamber was maintained at 37°C temperature, 5% CO₂ and supplemented with ENR media made with phenol red-free DMEM/F12. Three-dimension reconstruction was performed using Arivis Vision 4D. 3.0.1 software. For [Figure 1D](#) and [Video S2](#), the image was denoised using median filter (radius 1) followed by background correction.

Rab11DN and Rab7DN vector construction

Rab11DN and Rab7DN were generated by mutagenesis PCR from the pCMV-intron myc Rab11WT (Addgene #46785) and pCMV-SPORT6-Rab7, respectively.

Primers used for Rab11DN are: 5'-GTGTTGGAAAGAACAACCTCCTGTCTCGATTTA-3' & 5'-GACAGGAGGTTGTTCTTTCCAA CACCAGAATC-3'. Primers used for Rab7DN are: 5'- CTGGTGTGGAAAGAACTCTCATGAACCAG -3' & 5'- CTGGTTCATGAGA GAGTTCTTTCCAACACCAG -3'. DN constructs were cloned into the multiple cloning site I (MCSI) and mCerulean sequence was cloned into the MCS II of Tet-On® 3G Inducible Expression System (Bicistronic Version, pTRE3G-IRES, Takara # 631166)

Lentivirus production and concentration

Lentivirus particle containing tet-activator was purchased from Takara (#631311). Lentivirus containing inducible mycRab11DN-mCerulean and Rab7DN-mCerulean constructs were produced using calcium phosphate transfection in HEK293T cells (Takara # 631312, user protocol). 2nd generation lentiviral plasmids psPAX2 and pMD2.G were used (Addgene #12260, #12259). Lentivirus was concentrated with PEG-itTM (System Bioscience, # LV810A-1, user protocol).

Organoid transduction

Organoids were transduced with lentivirus using the method modified from Maru et al., 2016 and Van Lidth de Jeude et al., 2015^{11,12}. Briefly, 1st generation of organoids from the crypts were passed with ENR medium containing Wnt3a, CHIR99021 and Nicotinamide to enrich stem cell population. 2-3 days later when the organoids display spheroid morphology with few dead cells in the lumen, organoids were mechanically broken down and trypsinized to single cells. Cells were washed and supplemented with the Lentivirus concentrate in a final concentration of 1X ENR media containing Wnt 3a, CHIR99021, Nicotinamide, TransDuxMAXTM with enhancer. Cells and virus mixture were incubated at 37°C water bath for around 1 hour, distributed to a matrigel-coated 24 well plates, incubated in the 37°C incubator for overnight. The next day, as live cells settle on the coated matrigel, supernatant containing virus and dead cell debris was carefully removed and fresh matrigel was added to form a sandwich having the live cells in the center of the two layers of the matrigel. ENR medium containing Wnt3a, CHIR99021 and Nicotinamide (without TransDuxMAXTM) was supplied for 2 more days. A final concentration of 1 µg/ml puromycin and 100 µg/ml geneticin (neomycin) were added to select for the successful transduction with pTRE3G-DN mutant-IRES;mCerulean and tet-activator, respectively, until the transduced stem cells form small visible organoids. Media was returned to regular ENR media containing three antibiotics (pen-strep, puromycin and geneticin) and transduced organoids were cultured in presence of the three antibiotics throughout.

QUANTIFICATION AND STATISTICAL ANALYSIS

Statistical Analysis

All statistical analysis has been performed using Prism 8 (Graphpad). Details for statistical tests used can be found in figure legends, including the number of replicates performed and number of organoids analyzed for each condition and p value